J. Fluid Mech. (1988), *vol.* 188, *pp.* 411–435
Printed in Great Britain

The centring dynamics of a thin liquid shell in capillary oscillations

By CHUN P. LEE AND TAYLOR G. WANG
Jet Propulsion Laboratory, California Institute of Technology, Pasadena, CA 91103, USA

(Received 18 September 1986 and in revised form 17 August 1987)

The physical mechanism governing the centring of a hollow liquid shell in capillary oscillations, which has been observed in experiments, is investigated theoretically. First, the shell is assumed to be inviscid and to have a thickness that is much less than its spherical radius. A system of one-dimensional nonlinear equations of motion is derived using a thin-sheet model. From a numerical study the nonlinear effects of the wave are found to cause the core to oscillate slowly relative to the shell while the centre of mass of the whole system remains stationary. The effects of small viscosity are then considered in an approximation. Finally the strength of the centring mechanism is compared with that of the decentring effect due to buoyancy. The findings are consistent with the limited experimental information available.

1. Introduction

In recent years there has been much study of the dynamics of compound drops (Johnson & Sadhal 1985), motivated by an interest in producing capsules for inertial confinement fusion, and other potential applications (Lee *et al.* 1986). A compound drop consists of a fluid core enclosed within a fluid shell immersed in a fluid medium. Saffren, Elleman & Rhim (1982) found that a compound drop oscillates under the influence of surface tension like a coupled pair of pendula, with the sloshing mode in which the two interfaces move by 180° out of phase, and the bubble mode in which they move in phase.

Many experiments have indicated a tendency for a compound drop in oscillation to become concentric. In a zero-gravity experiment (using a NASA KC-135 aircraft), water droplets with injected air bubbles consistently assumed concentric spherical form (T. G. Wang and D. D. Elleman 1981, private communication). Free-falling hollow liquid shells, about 1 mm in radius, produced by annular jet instability, tended to remain concentric (Kendall 1986; Lee & Wang 1986). In an acoustic levitation experiment (Trinh 1983), the hollow shell produced by introduction of air into a 1 mm drop was found to resist breakup when oscillation was induced.

It has also been demonstrated (Saffren *et al.* 1982) in a neutral buoyancy tank that a compound drop formed of immiscible liquids becomes concentric when excited into oscillations. A similar effect has been seen (Lee *et al* 1982) when a layer of liquid coating a small solid sphere in acoustic levitation was forced into a capillary oscillation.

In this study we are interested in the first group of experiments, which involve hollow liquid shells. A shell experiences negligible viscous stress on its two interfaces, so that if the relevant Reynolds number is large (§6), viscosity is negligible. We shall find the viscous correction later. But even without viscosity the problem is not

trivial. According to a linear analysis (Saffron *et al.* 1982) the core sees a neutral potential inside the shell, implying that centring must be a nonlinear effect.

In the second group viscosity plays a dominant role in centring because viscous friction is strong, as is evident from the fact that an oil droplet can stay immersed just below a water surface for a long time. Even in the linear limit the core cannot see a neutral potential because the distribution of viscous stress must be affected by the uneven shell thickness. Consideration of nonlinearity is not necessary.

For the hollow liquid shell, if the shell thickness is much less than its mean radius we can model it as a thin sheet, reducing the problem to a one-dimensional one. In previous work (Lee & Wang 1986) we described the annular jet instability by a thin-sheet model, ignoring the flow structure across the sheet. In this work the model is amended to include a description of the variation in the shell thickness as the liquid translates along the sheet.

2. Qualitative description of the model

Let the origin of the coordinate system be chosen inside the thin liquid shell and assume axisymmetry. Polar coordinates (r, θ) will be used, but only θ will appear in the final form as a spatial coordinate.

Let us call the outer surface of the shell R_o and the inner one R_i. If we draw a line from the origin to the outer surface intersecting the inner surface at point P_i and the outer one at point P_o we can construct the midpoint Q between the two points (see figure 1), the locus of which is $R = \frac{1}{2}(R_o + R_i)$. In our thin-sheet model the position of the shell is defined by R as a function of θ. When the shell is spherical, concentric, and centred at the origin, R is a constant R_s regarded as the equilibrium radius of the shell, and the thickness of the shell is a constant, D_s. Let us define $\delta = D_s/R_s$. When the shell does not sit at the origin, R is a displaced spherical surface of radius R_s to a good approximation. In general R can be wavy and time dependent. At every point on the surface R we can construct a unit normal vector $\boldsymbol{n}$ pointing outward and a unit tangential vector $\boldsymbol{s}$ pointing in the increasing θ-direction (figure 1).

We need to specify the distribution of liquid around the shell. Let a normal to the surface R be drawn at Q, intersecting R_o at point Q_o and R_i at point Q_i (figure 1). The distance between Q_o and Q_i is called the thickness D of the shell there; and the product $\mu = \rho D$, where ρ is the density of the liquid, is called the surface density. In the spherical concentric case D equals D_s, and μ is just $\mu_s = \rho D_s$. The relation between (R, μ) and (R_o, R_i) is invertible.

The velocity distribution of the shell is described below. In the thin-shell limit the tangential velocity is almost uniform across the liquid layer; therefore in the model we assign to the shell a tangential velocity $v_s(\theta, t)$. In the physical shell, the normal velocity consists of one part representing the net translation of the shell in the normal direction, and the other the internal flow, which in general changes sign near the mid-surface of the shell. The former is taken to be the normal velocity $v_n(\theta, t)$ of the shell in the model. But the latter will be ignored since it does not carry a net normal momentum, and its magnitude is negligible in the thin-shell limit. The shell in the model therefore does not have an internal flow.

We assume that the gaseous core is incompressible, and that its pressure is uniform in space but in general dependent on time. The medium pressure, serving only as a reference level here, will be set to zero.

If the core pressure P is given, and if the two interfaces R_o and R_i are known we can evaluate the pressures p_o and p_i at any point immediately on the liquid side of

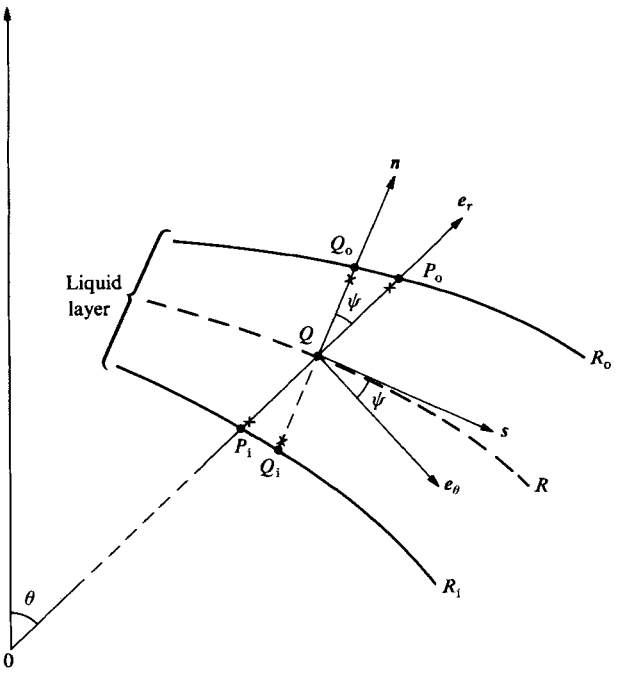

FIGURE 1. Basic quantities in the model. Given θ, p_o and p_i are evaluated at points marked by crosses near points P_o and P_i, whereas p_o^* and p_i^* are evaluated at points marked by crosses near Q_o and Q_i.

an interface. The pressure inside the liquid can then be considered to vary almost linearly across the small shell thickness. Let us define a mean pressure p at a point θ on R as $p = \frac{1}{2}(p_o^* + p_i^*)$, where the asterisks denote that the quantities are evaluated in the immediate neighbourhoods of the points Q_o and Q_i along the normal vector (figure 1), not the points P_o and P_i along the radial vector. The starred quantities can be derived from the non-starred ones using a Taylor-series expansion. Similarly the normal pressure difference Δq at θ on R is $\Delta q = p_i^* - p_o^*$. Furthermore, we can write $\Delta q = \Delta p + P$, where Δp means the part of Δq due directly to the distortions of the interfaces.

In deriving the momentum equations we have the tangential motion governed by the tangential gradient of p and the normal motion by Δq. We shall obtain the continuity equation for the mass flow in the shell. Full nonlinearity will be retained. To close the equations we shall obtain an explicit expression for P in terms of other quantities by using the assumptions about the core, and the normal momentum equation. Note that p and Δp are determined by R and μ, but that P is a functional of all of R, μ, v_s and v_n.

We shall solve the equations numerically for R, μ, v_s and v_n as an initial-value problem in a parameter study. The error involved in describing the shell using a thin-sheet model is essentially of the order of δ^2.

We have checked the performance of the thin-sheet model compared to that of the potential theory (Taylor 1959) in a study of the waves on a flat liquid sheet in the linear limit. Also, we have found that the same approach in the study of a thin liquid column leads to a well-known one-dimensional theory of the jet (Lee 1974).

3. Mathematical formulation

We shall use the modelling framework outlined in §2 to derive the following.

3.1. *Continuity equation*

Given R and μ as functions of θ at t, consider an axisymmetric elemental ring of the shell of width δs, lying between θ and $\theta+\delta\theta$ at a radial distance R from the origin. Conservation of mass of the elemental ring requires that

$$\frac{\mathrm{d}}{\mathrm{d}t}(2\pi R\mu \sin\theta\, \delta s) = 0, \tag{3.1}$$

where $\mathrm{d}/\mathrm{d}t$ means the convective derivative. From the product rule of differentiation the left-hand side of (3.1) can be split into four terms carrying $\mathrm{d}R/\mathrm{d}t$, $\mathrm{d}\mu/\mathrm{d}t$, $\mathrm{d}\theta/\mathrm{d}t$ and $\mathrm{d}\delta s/\mathrm{d}t$.

From geometrical and kinematic considerations we have

$$\frac{\mathrm{d}R}{\mathrm{d}t} = v_s \sin\psi + v_n \cos\psi, \tag{3.2}$$

and

$$R\frac{\mathrm{d}\theta}{\mathrm{d}t} = v_s \cos\psi - v_n \sin\psi, \tag{3.3}$$

where

$$\tan\psi = \frac{1}{R}\frac{\partial R}{\partial\theta}, \tag{3.4}$$

is the slope of the sheet at θ (figure 1).

To evaluate $\mathrm{d}\delta s/\mathrm{d}t$, let δs change to $\delta s'$ when t changes to $t+\delta t$. To find $\delta s'$ we need to know the s-component of the relative velocity between the two ends of δs; the n-component, being a higher-order correction, can be neglected. The velocity is given by $\partial \boldsymbol{v}/\partial\theta$ multiplied by the angle subtended by the two ends at the origin, where

$$\boldsymbol{v} = v_s \boldsymbol{s} + v_n \boldsymbol{n}. \tag{3.5}$$

Thus

$$\delta s' = \delta s + \boldsymbol{s}\cdot\frac{\partial \boldsymbol{v}}{\partial\theta}\frac{\delta s\cos\psi}{R}\delta t, \tag{3.6}$$

in which the fraction preceding δt on the right-hand side is the angle just mentioned. Noting that

$$\boldsymbol{s} = \sin\psi\, \boldsymbol{e}_r + \cos\psi\, \boldsymbol{e}_\theta, \tag{3.7}$$

and

$$\boldsymbol{n} = \cos\psi\, \boldsymbol{e}_r - \sin\psi\, \boldsymbol{e}_\theta, \tag{3.8}$$

we can calculate $\partial \boldsymbol{v}/\partial\theta$ using (3.5), substitute the result into (3.6) and, after using (3.4), obtain

$$\frac{\mathrm{d}\delta s}{\mathrm{d}t} = \frac{\delta s'-\delta s}{\delta t} = \delta s\frac{\cos\psi}{R}\left\{\frac{\partial v_s}{\partial\theta} + v_n - v_n\cos^2\psi\left[\frac{1}{R}\frac{\partial^2 R}{\partial\theta^2} - \frac{1}{R^2}\left(\frac{\partial R}{\partial\theta}\right)^2\right]\right\}. \tag{3.9}$$

The last derivatives $\mathrm{d}\mu/\mathrm{d}t$ is written directly from the definition of $\mathrm{d}/\mathrm{d}t$, using the fact that the system has no dependence on the radial coordinate r:

$$\frac{\mathrm{d}\mu}{\mathrm{d}t} = \frac{\partial\mu}{\partial t} + [v_s\cos\psi - v_n\sin\psi]\frac{1}{R}\frac{\partial\mu}{\partial\theta}, \tag{3.10}$$

where the quantity inside the bracket on the right-hand side is identified as the component of $\boldsymbol{v}$ in the θ-direction.

Putting all the derivatives (3.2), (3.3), (3.9) and (3.10) into (3.1), after some algebra, we have

$$\frac{\partial \mu}{\partial t} = -\frac{K}{R}\frac{\partial \mu}{\partial \theta} - \frac{\mu}{R}\left[\cos\psi \frac{\partial v_s}{\partial \theta} + f_v \cos\psi + v_s \sin\psi\right] - \mu C v_n, \tag{3.11}$$

where

$$K = v_s \cos\psi - v_n \sin\psi, \tag{3.12}$$

$$f_v = \begin{cases} \dfrac{v_s \cos\theta}{\sin\theta} & \text{for } 0 < \theta < \pi, \\ \dfrac{\partial v_s}{\partial \theta} & \text{for } \theta = 0 \quad \text{or } \pi, \end{cases} \tag{3.13}$$

and

$$C = \frac{1}{R}\left[2\cos\psi + \sin^2\psi \cos\psi - f - \frac{\cos^3\psi}{R}\frac{\partial^2 R}{\partial \theta^2}\right], \tag{3.14}$$

in which

$$f = \begin{cases} \dfrac{\sin\psi \cos\theta}{\sin\theta} & \text{for } 0 < \theta < \pi, \\ \dfrac{\partial^2 R/\partial \theta^2}{R} & \text{for } \theta = 0 \quad \text{or } \pi. \end{cases} \tag{3.15}$$

Here K is the θ-component of $\boldsymbol{v}$ arising from the convective derivative $\mathrm{d}/\mathrm{d}t$ defined in (3.10). C has the meaning of the curvature of the surface defined by R. The functions f and f_v are well-behaved in θ in the interval $[0, \pi]$.

3.2. *Kinematic relation*

We need a relation between $\partial R/\partial t$ and $\boldsymbol{v}$. Because we have defined the coordinates (s, n) in such a way that $\boldsymbol{s}$ lies in the tangential direction of the curve R, v_s does not contribute to the rate of change of R with t. Then it is obvious from geometrical and kinematic considerations that

$$\frac{\partial R}{\partial t} = \frac{v_n}{\cos\psi}. \tag{3.16}$$

3.3. *Momentum equations*

Applying Newton's second law to the elemental ring and using the forces discussed in §2 we have

$$\frac{\mathrm{d}}{\mathrm{d}t}(2\pi R \mu \boldsymbol{v} \sin\theta\, \delta s) = 2\pi R \sin\theta\, \delta s\left(-\frac{\mu \cos\psi}{\rho R}\frac{\partial p}{\partial \theta}\boldsymbol{s} + \Delta q\, \boldsymbol{n}\right), \tag{3.17}$$

where the first term inside the bracket on the right-hand side is proportional to the tangential gradient of p, and the second one is the total normal pressure. Using (3.1), the factor $2\pi R\mu \sin\theta\, \delta s$ on the left-hand side of (3.17) commutes with $\mathrm{d}/\mathrm{d}t$ and can be factored out, leaving (3.17) as

$$\mu \frac{\mathrm{d}\boldsymbol{v}}{\mathrm{d}t} = -\frac{\mu \cos\psi}{\rho R}\frac{\partial p}{\partial \theta}\boldsymbol{s} + \Delta q\, \boldsymbol{n}. \tag{3.18}$$

To evaluate $\mathrm{d}\boldsymbol{v}/\mathrm{d}t$ on the left-hand side we substitute $\boldsymbol{s}$, as defined in (3.7), and $\boldsymbol{n}$, as defined in (3.8), into (3.5), apply the operation $\mathrm{d}/\mathrm{d}t$ given in (3.10) (ignoring μ there),

use the definition of ψ given in (3.4) and involve the kinematic condition given in (3.16). The resulting equation can be separated into the s- and n-components:

$$\frac{\partial v_s}{\partial t} = -\frac{K}{R}\frac{\partial v_s}{\partial \theta} - v_n H - \lambda_1 \frac{\cos\psi}{\rho R}\frac{\partial p}{\partial \theta}, \tag{3.19}$$

$$\frac{\partial v_n}{\partial t} = -\frac{K}{R}\frac{\partial v_n}{\partial \theta} + v_s H + \frac{\lambda_1}{\mu}[P + \Delta p]. \tag{3.20}$$

Here K has been defined in (3.12); H represents curvilinear effects, i.e. those due to the time-dependence of $\boldsymbol{s}$ and $\boldsymbol{n}$:

$$H = \frac{K}{R} - \frac{\cos\psi}{R}\frac{\partial v_n}{\partial \theta} + \frac{\cos\psi \sin\psi}{R}(v_s \sin\psi + v_n \cos\psi) - \frac{v_s \cos^3\psi}{R^2}\frac{\partial^2 R}{\partial \theta^2} + \frac{v_n \sin^3\psi}{R}. \tag{3.21}$$

The coefficient λ_1 is taken to be unity for the present but will take on other values when we make the equations dimensionless.

3.4. *The derivation of p and Δp*

In the following we shall consider R and μ as given in the evaluation of p and Δp.

In figure 1 the distance D_a between the points P_o and P_i is $D/\cos\psi$. Therefore with Q defined as the midpoint between P_o and P_i and the relation between D and μ. we have

$$R_o = R + \frac{\mu}{2\rho \cos\psi}, \tag{3.22}$$

and

$$R_i = R - \frac{\mu}{2\rho \cos\psi}. \tag{3.23}$$

Following (3.14) we have the curvature C_o of the outer surface R_o and C_i of the inner surface R_i respectively given by

$$C_o = \frac{1}{R_o}\left[2\cos\psi_o + \sin^2\psi_o \cos\psi_o - f_o - \frac{\cos^3\psi_o}{R_o}\frac{\partial^2 R_o}{\partial \theta^2}\right], \tag{3.24}$$

$$C_i = \frac{1}{R_i}\left[2\cos\psi_i + \sin^2\psi_i \cos\psi_i - f_i - \frac{\cos^3\psi_o}{R_i}\frac{\partial^2 R_o}{\partial \theta^2}\right]; \tag{3.25}$$

where, as in (3.4), we have defined

$$\tan\psi_{o,i} = \frac{1}{R_{o,i}}\frac{\partial R_{o,i}}{\partial \theta}; \tag{3.26}$$

and similarly, as in (3.15), we have defined

$$f_{o,i} = \begin{cases} \dfrac{\sin\psi_{o,i}\cos\theta}{\sin\theta} & \text{for } 0 < \theta < \pi, \\ \dfrac{\partial^2 R_{o,i}/\partial\theta^2}{R_{o,i}} & \text{for } \theta = 0 \quad \text{or } \pi. \end{cases} \tag{3.27}$$

Here and in the rest of this work the subscript 'o, i' denotes 'the outer or the inner surface'. Then we can write down p_o and p_i, from consideration of the boundary

condition pertaining to the normal stress, at each of the two interfaces of the physical shell, as

$$p_o = \sigma C_o, \tag{3.28}$$

and

$$p_i = -\sigma C_i + P. \tag{3.29}$$

The corresponding p_o^* and p_i^* are given by

$$p_o^* = \sigma C_o^*, \tag{3.30}$$

and

$$p_i^* = -\sigma C_i^* + P, \tag{3.31}$$

where the asterisks signify that the quantities are evaluated at the positions explained in §2.

We wish to find explicit expressions for p_o^* and p_i^* by relating them to p_o and p_i. Equivalently, we need to express C_o^* and C_i^* in terms of C_o and C_i. Let point Q_o be at angle $\theta - \delta\theta_o$, and Q_i be at $\theta + \delta\theta_i$ in figure 1. Then applying Taylor-series expansions we obtain

$$C_{o,i}^* = C_{o,i} \mp \frac{\partial C_{o,i}}{\partial \theta}\delta\theta_{o,i} + \frac{1}{2}\frac{\partial^2 C_{o,i}}{\partial \theta^2}(\delta\theta_{o,i})^2. \tag{3.32}$$

In this equation and in some of what will follow we keep terms up to $O(\delta^2)$ because we expect cancellations at lower orders in certain manipulations.

To find $\delta\theta_o$ and $\delta\theta_i$ we need the following. Let D_0 be the distance between Q and Q_o, and D_i be that between Q and Q_i, such that their sum is the local thickness D. It is easy to see that

$$\delta\theta_{o,i} = \frac{D_{o,i}\sin\psi}{R \pm D_{o,i}\cos\psi} = \frac{D_{o,i}\sin\psi}{R}\left(1 \mp \frac{D_{o,i}\cos\psi}{R}\right), \tag{3.33}$$

in which we have used the fact that D is much less than R. This in turn requires us to find D_o and D_i.

Referring to figure 2, which shows some other details of the same part of the shell drawn in figure 1, we note that

$$D_{o,i} = \tfrac{1}{2}D_a \cos\psi\,(1 \mp \tan\psi\,\tan\beta_{o,i}), \tag{3.34}$$

where $\tan\beta_o$ and $\tan\beta_i$ are the slopes of R_o and R_i relative to R there.

The values of $\tan\beta_o$ and $\tan\beta_i$ are found as follows. If θ is increased by $\delta\theta$, there is a corresponding displacement $R\delta\theta/\cos\psi$ along the surface R, leading to a new position where $D_{o,i}$ changes by $(\partial D_{o,i}/\partial\theta)\,\delta\theta$. Therefore

$$\tan\beta_{o,i} = \frac{\partial D_{o,i}}{\partial\theta}\frac{\cos\psi}{R}. \tag{3.35}$$

Substituting (3.35) into the right-hand side of (3.34), iterating for $D_{o,i}$, using the definition $\mu_{o,i} = \rho D_{o,i}$ and recalling the meaning of D_a we have

$$\mu_{o,i} = \tfrac{1}{2}\mu\left(1 \mp \frac{\sin\psi}{2\rho R}\frac{\partial\mu}{\partial\theta}\right). \tag{3.36}$$

Using (3.36), (3.33) and the relation between μ's and D's we can obtain the expressions for $C_{o,i}^*$ in (3.32) in terms basically of R and μ. Then we can find $p_{o,i}^*$ in (3.30) and (3.31) explicitly to the second order in δ. Instead of writing them here, we evaluate p and Δp:

$$p = \tfrac{1}{2}\sigma\left[C_o - C_i - \frac{\partial C}{\partial\theta}\frac{\mu\sin\psi}{\rho R}\right] + \tfrac{1}{2}P, \tag{3.37}$$

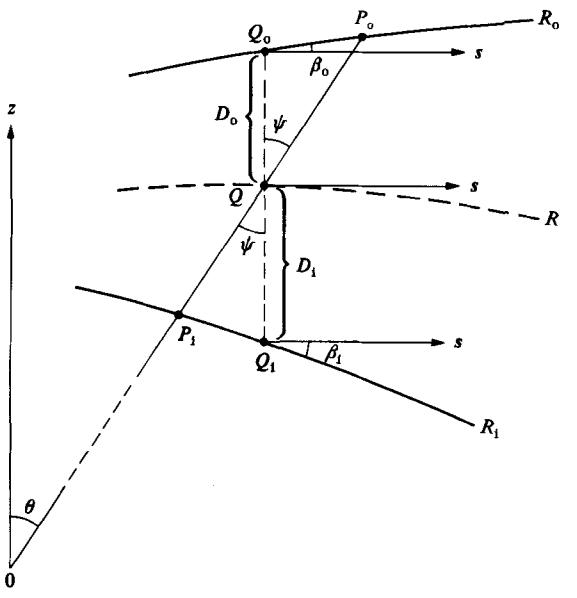

FIGURE 2. Geometry pertaining to (3.34) in the calculation of pressure.

and

$$\Delta p = \sigma\left[-(C_0+C_i)+\frac{\sin\psi}{\rho R}\left(\mu_0\frac{\partial C_0}{\partial\theta}-\mu_i\frac{\partial C_i}{\partial\theta}\right)-\frac{\partial C}{\partial\theta}\frac{\mu^2\sin\psi\cos\psi}{2\rho^2R^2}-\left(\frac{\mu\sin\psi}{2\rho R}\right)^2\frac{\partial^2 C}{\partial\theta^2}\right]. \tag{3.38}$$

3.5. *Conservation of mass and volume*

Conservation of mass of the shell is expressed by

$$M = 2\pi\int_0^\pi \mathrm{d}\theta\sin\theta\frac{\mu R^2}{\cos\psi} = 4\pi R_s^2\mu_s \tag{3.39}$$

being constant.

Similarly, conservation of volume of the core is given by

$$V = \frac{2\pi}{3}\int_0^\pi \mathrm{d}\theta\sin\theta R^3 = \tfrac{4}{3}\pi R_s^3 \tag{3.40}$$

being constant.

3.6. *The core pressure P*

To derive P we first consider the incompressibility of the core. Differentiating (3.40) by t we obtain

$$\int_0^\pi \mathrm{d}\theta\sin\theta R^2\frac{\partial R}{\partial t} = 0. \tag{3.41}$$

A second differentiation with respect to t, and use of the kinematic equation (3.16) gives

$$\int_0^\pi \mathrm{d}\theta\sin\theta R^2\frac{\partial^2 R}{\partial t^2} = -2\int_0^\pi \mathrm{d}\theta\sin\theta\frac{Rv_n^2}{(\cos\psi)^2}. \tag{3.42}$$

We then have to consider the kinematic condition (3.16). Using (3.4) and (3.16) we obtain

$$\frac{\partial v_n}{\partial t} = \frac{\partial^2 R}{\partial t^2}\cos\psi - \frac{v_n \sin\psi}{R}\frac{\partial v_n}{\partial \theta} - \frac{v_n^2}{R^2} - \sin^2\psi\cos\psi\frac{\partial^2 R}{\partial \theta^2} + \frac{v_n^2 \sin^2\psi}{R\cos\psi}(1+\sin^2\psi). \tag{3.43}$$

Next we consider the normal momentum equation (3.20). We move P to the left-hand side and everything else to the right-hand side, multiply both sides by $R^2/(\mu\cos\psi)$ and integrate over θ from 0 to π. On the left-hand we use the assumption that P is uniform in space and take it out of the integral sign. On the right-hand side the integrand contains $\partial v_n/\partial t$, and that is where we can use (3.43) and (3.42) successively.

Finally after rearranging terms and using (3.21) we have

$$P = \frac{\int_0^\pi \mathrm{d}\theta \sin\theta F}{\int_0^\pi \mathrm{d}\theta \sin\theta \dfrac{R^2}{\mu\cos\psi}}, \tag{3.44}$$

where

$$F = \lambda_2\left[\frac{2RK}{\cos\psi}\frac{\partial v_n}{\partial\theta} + (v_s^2\cos^2\psi - v_n^2\sin^2\psi)\frac{\partial^2 R}{\partial\theta^2} - Rv_s^2(1+\sin^2\psi) - Rv_n^2(2+\sin^2\psi)\right] - \frac{R^2\Delta p}{\mu\cos\psi}, \tag{3.45}$$

in which λ_2 is unity for the time being but will be assigned values when we make the equations dimensionless.

3.7. *Conservation of energy*

The energy of the shell consists of the kinetic energy E_K of the liquid, the potential energy $(E_\mathrm{P})_\mathrm{s}$ due to variation in thickness of the shell, and the potential energy $(E_\mathrm{P})_\mathrm{b}$ due to distortion of the shell from sphericity. Both potential energies are associated with changes in the total surface area of the interfaces and exist because of surface tension. The total energy must be conserved in the absence of an external force.

In the thin sheet model the kinetic energy is

$$E_\mathrm{K} = \pi\lambda_2\int_0^\pi \mathrm{d}\theta \sin\theta \frac{R^2\mu(v_s^2+v_n^2)}{\cos\psi}, \tag{3.46}$$

in which λ_2 is the same as that in (3.45). The potential energy $(E_\mathrm{P})_\mathrm{b}$, ignoring the shell finite thickness, is

$$(E_\mathrm{P})_\mathrm{b} = 4\pi\sigma\int_0^\pi \mathrm{d}\theta\sin\theta\frac{R^2}{\cos\psi} - 8\pi\sigma R_\mathrm{s}^2. \tag{3.47}$$

On the right-hand side we have included a factor of 2 because the shell has two interfaces.

To account for the energy due to the unevenness in thickness of the shell we need to consider both the outer and inner surfaces. The outer/inner surface has an area of

$$A_{\mathrm{o,i}} = 2\pi\int_0^\pi \mathrm{d}\theta\sin\theta\frac{R_{\mathrm{o,i}}^2}{\cos\psi_{\mathrm{o,i}}}, \tag{3.48}$$

containing a volume of

$$V_{o,i} = \tfrac{2}{3}\pi \int_0^\pi d\theta \sin\theta R_{o,i}^3. \tag{3.49}$$

In these two equations $R_{o,i}$ is given by (3.22) or (3.23), in which μ is not a constant in θ in general.

Imagine that we now smooth out the 'wrinkle' on the surface $R_{o,i}$ by replacing $\frac{1}{2}\mu$ with $\nu_{o,i}$ which is constant in θ (but depends on t in general), while preserving its volume $V_{o,i}$. The surface then becomes

$$S_{o,i} = R \pm \frac{\nu_{o,i}}{\rho \cos\psi}; \tag{3.50}$$

and the surface area is reduced to

$$B_{o,i} = 2\pi \int_0^\pi d\theta \sin\theta \frac{S_{o,i}^2}{\cos\psi}; \tag{3.51}$$

but the volume maintains the same value

$$V_{o,i} = \tfrac{2}{3}\pi \int_0^\pi d\theta \sin\theta S_{o,i}^3, \tag{3.52}$$

although the integral on the right-hand side has a different integrand. Equating the right-hand sides of (3.49) and (3.52), using (3.50) and the fact that $\nu_{o,i}$ is constant in θ, we obtain a cubic algebraic equation in $\nu_{o,i}$ which can be solved readily for a real positive root. Substituting the value of $\nu_{o,i}$ into (3.50), we can find $B_{o,i}$ in (3.51).

The potential $(E_P)_s$ is finally defined as the gain in surface energy when the shell goes from an 'unwrinkled' state to a 'wrinkled' one:

$$(E_P)_s = \sigma(A_o - B_o + A_i - B_i). \tag{3.53}$$

The total energy is a constant of motion given by

$$E = E_K + (E_P)_b + (E_P)_s. \tag{3.54}$$

3.8. *Centre of mass and geometrical centre*

In the absence of an external force the centre of mass, given by

$$Z_{cm} = \frac{2\pi}{M} \int_0^\pi d\theta \sin\theta \frac{R^3 \mu \cos\theta}{\cos\psi}, \tag{3.55}$$

is stationary in space. But the geometrical centre of the shell, defined as

$$Z = \frac{\int_0^\pi d\theta \sin\theta \dfrac{R^3 \cos\theta}{\cos\psi}}{\int_0^\pi d\theta \sin\theta \dfrac{R^2}{\cos\psi}}, \tag{3.56}$$

can move as the liquid in motion adjusts itself in such a way as to maintain Z_{cm} constant. Let $Z_s = Z - Z_{cm}$, the position of the geometrical centre relative to the fixed centre of mass. In this work the centring condition of the shell is monitored by following the time-evolution of Z_s.

3.9. *Initial and boundary conditions*

The problem is considered to be an initial-value problem in t for $t > 0$, and a boundary-value problem in θ for θ from 0 to π. With the equations primarily defined

by (3.11), (3.16), (3.19), (3.20) and (3.44) the unknown functions to be solved for are R, μ, v_s and v_n.

The boundary conditions defined at $\theta = 0$ and π are

$$\frac{\partial R}{\partial \theta} = \frac{\partial \mu}{\partial \theta} = \frac{\partial v_n}{\partial \theta} = v_s = 0, \tag{3.57}$$

which simply reflect the symmetry of the system at the two points.

For the sloshing mode the shell motion starts with a non-uniform distribution of surface density. Thus for θ from 0 to π the initial conditions are

$$R = R_s, \tag{3.58a}$$

$$\mu = \mu_s[1 - \Delta \cos\theta + \epsilon P_n(\cos\theta)], \tag{3.58b}$$

and

$$v_s = v_n = 0, \tag{3.58c}$$

where in (3.58b) ϵ and Δ represent the initial disturbance and core displacement respectively, and P_n is a Legendre polynomial.

The bubble mode of oscillation occurs when the shell starts with a non-spherical form. The corresponding initial conditions are

$$R = R_s' + \epsilon R_s P_n(\cos\theta), \tag{3.59a}$$

$$\mu = \mu_s'(1 - \Delta \cos\theta), \tag{3.59b}$$

and

$$v_s = v_n = 0, \tag{3.59c}$$

for θ from 0 to π, where ϵ and Δ represent the initial distortion and core displacement respectively, and R_s' and μ_s' are determined as follows. R_s' is calculated by requiring that (3.59a) satisfy the conservation law for the core volume defined by (3.40). Using this value of R_s' we substitute (3.59a) and (3.59b) into (3.39) to find the value of μ_s' which is consistent with the conservation law for the shell mass.

4. Linear analysis

Let us consider a thin concentric liquid shell placed at the origin. In equilibrium the core pressure P is $4\sigma/R_s$, balancing an inward-pointing pressure force due to the surface tension of the shell given by $-\Delta p = 4\sigma/R_s$.

Consider now that the shell is under infinitesimal disturbance:

$$R = R_s + R', \quad \mu = \mu_s + \mu' \tag{4.1a, b}$$

$$v_s = v_s', \quad v_n = v_n'. \tag{4.1c, d}$$

The disturbance falls into either of two types: the sloshing mode or the bubble mode.

4.1. *Sloshing mode*

In this case the liquid essentially shuffles back and forth in the tangential direction. The normal movement of the shell can be neglected. Therefore we let v_n' and R' be zero, and $\tan\psi$ in (3.4) is also zero.

Using (3.22)–(3.25) we find that Δp in (3.38) is equal to $-4\sigma/R_s$ with an error of the order of at most δ^2. Substituting this result into (3.44) we find that P is $4\sigma/R_s$ plus a similar error. Neglecting errors of this magnitude we find that Δp and P cancel each other just as they do in the equilibrium situation. It follows that the right-hand side of the normal momentum equation (3.20) is zero with an error of $O(\delta^2)$,

reaffirming our assumption that v_n' is zero. Thus the right-hand side of (3.16) is also zero, reaffirming our other assumption that R' is zero. Using (3.22)–(3.25) and (3.37) to obtain the mean pressure p, and substituting the result into the tangential momentum equation (3.19), we find

$$\frac{\partial v_s'}{\partial t} = -\frac{\sigma}{2\rho^2 R_s^3}\frac{\partial}{\partial\theta}(\mathrm{L}^2-2)\,\mu', \tag{4.2a}$$

where L^2 is the operator

$$\mathrm{L}^2 = -\frac{1}{\sin\theta}\frac{\partial}{\partial\theta}\left(\sin\theta\frac{\partial}{\partial\theta}\right)$$

for which the eigenfunctions are the Legendre polynomials $\{P_n\}$ with the corresponding eigenvalues $\{n(n+1)\}$. The continuity equation (3.11) yields

$$\frac{\partial\mu'}{\partial t} = -\frac{\mu_s}{R_s}\left[\frac{1}{\sin\theta}\frac{\partial}{\partial\theta}(\sin\theta\, v_s')\right]. \tag{4.2b}$$

Differentiating (4.2b) with respect to t and substituting (4.2a) we obtain the wave equation

$$\frac{\partial^2\mu'}{\partial t^2} = -\frac{\mu_s\sigma}{2\rho^2 R_s^4}\mathrm{L}^2(\mathrm{L}^2-2)\,\mu'. \tag{4.3}$$

By assuming a solution

$$\mu' = \epsilon\mu_s\cos\omega t P_n, \tag{4.4}$$

in accordance with (3.58b), we find that

$$\omega = \omega_0\,(\tfrac{1}{2}\delta)^{\frac{1}{2}}[n(n+1)\,(n-1)\,(n+2)]^{\frac{1}{2}}, \tag{4.5}$$

where $\omega_0 = (\sigma/\rho R_s^3)^{\frac{1}{2}}$. The corresponding v_s' can be found by substituting (4.4) into (4.2a):

$$v_s' = -\frac{\epsilon\omega R_s}{n(n+1)}\sin\omega t\frac{\partial P_n}{\partial\theta}. \tag{4.6}$$

4.2. *Bubble mode*

In this case normal motion is dominant in the shell, although some tangential motion is inevitable.

From (3.22)–(3.25), (3.38) and (3.44) we find that the static components of Δp and P cancel each other as before, but there remains a dynamic part due to the distortion of the shell. Equation (3.20) becomes, in the linear limit neglecting error of the order of δ^2,

$$\frac{\partial v_n'}{\partial t} = -\frac{2\sigma}{\mu_s R_s^2}(\mathrm{L}^2-2)\,R'. \tag{4.7}$$

The kinematic condition (3.16) immediately gives

$$\frac{\partial R'}{\partial t} = v_n'. \tag{4.8}$$

These two equations can be used to solve for v_n' and R'. But μ' is coupled to v_n' through the continuity equation (3.11):

$$\frac{\partial\mu'}{\partial t} = -\frac{\mu_s}{R_s}\left[\frac{1}{\sin\theta}\frac{\partial}{\partial\theta}(\sin\theta\, v_s')\right] - \frac{2\mu_s v_n'}{R_s}, \tag{4.9}$$

which differs from (4.2*b*) by an additional term at the end of the right-hand side. Consequently v_s' is also non-zero because of the tangential equation (3.19) which is reduced to (4.2*a*) again.

From (4.7) and (4.8) we find the wave equation

$$\frac{\partial^2 R'}{\partial t^2} = -\frac{2\sigma}{\mu_s R_s^2}(L^2-2)\,R'. \tag{4.10}$$

Assuming a solution of the form

$$R' = \epsilon R_s \cos\omega t\, P_n, \tag{4.11}$$

we find that

$$\omega = \frac{\omega_0}{(\frac{1}{2}\delta)^{\frac{1}{2}}}[(n-1)(n+2)]^{\frac{1}{2}}. \tag{4.12}$$

Substituting (4.11) into (4.8) we have

$$v_n' = -\omega\epsilon R_s \sin\omega t\, P_n. \tag{4.13}$$

Using these results we can find from (4.9), after neglecting terms of $O(\delta^2)$, that

$$\mu' = -2\epsilon\mu_s \cos\omega t\, P_n, \tag{4.14a}$$

and from (4.2*a*) that

$$v_s' = (\tfrac{1}{2}\delta^2\,\epsilon\omega R_s)\sin\omega t\,\frac{\partial P_n}{\partial\theta}. \tag{4.14b}$$

The natural frequencies given in (4.5) and (4.12) can be shown to agree with those from the potential theory (Saffren *et al.* 1982) with errors of $O(\delta^2)$.

Before closing this Section let us see how the above results obey the conservation laws (3.39), (3.40) and (3.54). The results for the sloshing mode do so with errors of $O(\delta^2)$. For the bubble mode, however, we need first to correct (4.1*a*) by replacing R_s with R_s' and determine the latter by using the conservation of volume equation (3.40) (see 3.59*a*). It is found that R_s' differs from R_s by a fraction of $O(\epsilon^2)$, which is nonlinear and was justifiably neglected earlier. But this difference is crucial in showing that the sum of E_K and $(E_P)_b$ is conserved, neglecting $(E_P)_s$ with an error of $O(\delta^2)$. Using this R_s', (4.1*b*) obeys conservation of mass (3.39) if we correct μ_s by an amount of $O(\epsilon^2)$.

5. Numerical work and results

5.1. *Dimensionless forms*

For numerical work we scale lengths by R_s, and μ by μ_s. Considering the ratio of $O(\delta)$ between the frequencies for the sloshing (4.5) and the bubble (4.12) modes, we assign to them different timescales: $1/\omega_s$ where $\omega_s = \omega_0\,\delta^{\frac{1}{2}}$, and $1/\omega_b$ where $\omega_b = \omega_0/\delta^{\frac{1}{2}}$, respectively. Dimensionless equations can be obtained conveniently by replacing $1/\rho$ by δ, and σ, R_s and μ_s by 1. For the sloshing mode we let λ_1 be $1/\delta^2$, and λ_2 be δ^2. For the bubble mode we let both be 1. The problem depends on three dimensionless parameters: the amplitude ϵ, the displacement Δ, both lying between 0 and 1, and the thickness δ which is much less than 1.

For the sloshing mode in the tangential momentum equation the pressure gradient is of $O(\epsilon)$, which drives the oscillations in v_s and μ, which are then both of $O(\epsilon)$. In the normal momentum equation Δp is $-4/\delta^2 + O(\epsilon^2)$ while P is $4/\delta^2 + O(\epsilon^2)$; their sum is

thus of $O(\epsilon^2)$. P enforces the incompressibility of the core but is otherwise inactive. Δp, without the large constant component, cannot excite much motion. Therefore if the shell is concentric the effect of Δp is negligible. The curvilinear term $v_s H$ in the same equation is roughly v_s^2/R, i.e. also of $O(\epsilon^2)$. But when the shell is non-concentric, both Δp and $v_s H$ become asymmetric, giving a net force of $O(\Delta\epsilon^2)$ leading to a slow translation of the shell. Then the tangential pressure gradient must play an additional role of redistributing the liquid in order to keep the centre of mass stationary.

For the bubble mode, in the normal momentum equation Δp is $-4+O(\epsilon)$, whereas P is $4+O(\epsilon^2)$ such that their sum is of $O(\epsilon)$. P again keeps the volume constant. Δp without the constant part drives the normal shell motion such that v_n and the oscillating part of R are of $O(\epsilon)$. The oscillation in μ is of $O(\epsilon)$ according to (4.14a). Then the tangential pressure gradient is of $O(\delta^2\epsilon)$. In the tangential momentum equation the curvilinear term $-v_n H$ is roughly $(1/R)(\partial/\partial\theta)(\frac{1}{2}v_n^2)$, i.e. of $O(\epsilon^2)$, such that when ϵ is larger than δ^2 it dominates the tangential pressure gradient. When the shell is non-concentric this term is of $O(\Delta\epsilon^2)$ causing the liquid to drift tangentially in one direction. Then Δp plays the additional role of repositioning the shell to keep the centre of mass fixed.

In our earlier work (Lee & Wang 1986) the equations are akin to those of the bubble mode, but they include no tangential pressure gradient. As we have just seen, when the wave amplitude is large the latter is negligible, justifying the previous approximation.

5.2. *Numerical procedure*

Since we have a fully nonlinear system here the question of numerical stability is not easy to answer. Therefore the choice of the numerical procedure is mostly heuristic. The spatial grid is formed by dividing the range $[0,\pi]$ of θ into equal parts. Integration in θ is done by the Simpson rule. Derivatives with respect to θ are expressed by central differences with exceptions described later. Integration in t is done by fourth-order Runge–Kutta method with a possible modification also described later. Note that computer time is not a concern because we carried out the calculation on a personal computer.

The performance of the program is checked by seeing that (a) the program can reproduce the linear results described in §4 when the wave amplitudes are small; (b) the conservation laws (3.39), (3.40) and (3.54) are satisfied at all times; (c) the results for a shell in oscillation are independent of the choice of the origin, provided that the origin is not far from its geometrical centre; (d) the centre of mass remains stationary at all times; and (e) a non-concentric stationary shell remains stationary irrespective of the choice of the origin.

To satisfy condition (a), we first smooth the functions f in (3.15), f_v in (3.13), and $f_{o,i}$ in (3.27) at $\theta = 0$ or π where they have removable singularities, by interpolation, making use of the boundary conditions (3.57) and the symmetry properties of the system there. Moreover, given the spatial step $\Delta\theta$, the choice of the time step Δt depends on the mode of oscillation. From the linear theory the wave equation (4.3) for the sloshing mode is biharmonic, involving a second derivative in t and a fourth derivative in θ. On the other hand (4.10) for the bubble mode involves second derivatives in both t and θ. Therefore the time step for the sloshing mode and the bubble mode should be of $O(\Delta\theta^2)$ and $O(\Delta\theta)$, respectively, the integration for the former being much slower. Furthermore, for stability the Runge–Kutta method has

to be modified for the sloshing mode by rewriting the first step of the four-step method as

$$y_{i,j+1} = \tfrac{1}{2}(y_{i-1,j} + y_{i+1,j}) + \left(\frac{\partial y}{\partial t}\right)_{i,j} \tfrac{1}{2}\Delta t,$$

where y means R, μ, v_s or v_n, and i and j denote spatial and temporal points. For the bubble mode no modification is necessary. After implementing these we can reproduce the linear results which also satisfy condition (*b*).

When the shell in oscillation is concentric but displaced from the origin, its geometrical centre and centre of mass both drift slowly in time, violating conditions (*c*) and (*d*). One reason is that although the spatial grid points are equally spaced in the interval $[0, \pi]$, they are actually not so on the surface of a displaced shell even if the shell is perfectly spherical. To remedy this we correct the central-difference scheme. The representation for $\partial y/\partial\theta$ can be shown to the second order to be

$$\frac{y_{i+1} - y_{i-1}}{2\Delta\theta} = \frac{\partial y}{\partial\theta} + \frac{1}{6}\frac{\partial^3 y}{\partial\theta^3}\Delta\theta^2.$$

By representing the second term on the right using the usual central difference and moving it to the left, we have a representation of $\partial y/\partial\theta$ to $O(\Delta\theta^2)$. Similarly we can obtain $\partial^2 y/\partial\theta^2$ to $O(\Delta\theta^2)$. In practice, we find by some testing that only $\partial R_{0,i}/\partial\theta$, $\partial^2 R_{0,i}/\partial\theta^2$, and $\partial p/\partial\theta$ need the correction. After doing so for the concentric shell, the geometrical centre no longer drifts relative to the centre of mass, but the latter still drifts. More generally, for the non-concentric shell the geometrical centre may drift, but the centre of mass also drifts in violation of condition (*d*). When it drifts too far the program suffers as shown by the increasing errors in the conservation laws.

An error inevitably arises from the asymmetry about the origin because of the way that we have defined R. As a remedy we impose a uniform artificial acceleration $a_c = -2|\Delta z|/\Delta t^2$ on the shell to cancel the drifting tendency, where Δz is the displacement of the centre of mass in the preceding time step. It turns out that a_c and its cumulative displacement are both small at all times. In general a_c cannot cause any side effect because without it the results are practically unchanged except for the drifting. By preventing the drift, to satisfy condition (*d*), the program can run longer.

Finally, for condition (*e*) the shell sits still for about a cycle or so before some instability leads to large errors. The program is designed to deal with either a sloshing or a bubble mode but not both. When $\epsilon = 0$ it fails because it finds both in the background noise. We choose to ignore this problem since the shell can stay still long enough to show a steady state. Also for the case of a shell in oscillation this kind of instability does not appear.

5.3. *Numerical results*

In the nonlinear regime the disturbance which is initially represented by a Legendre polynomial becomes only approximately periodic in time, even if the shell is concentric and centred at the origin. No matter how long we let the iteration continue, exact periodicity never occurs. This is not surprising, for it frequently happens when a nonlinear wave equation is treated numerically as an initial-value problem (Zabusky 1984). Here we shall overlook this irregularity, being more interested in the centring behaviour of the shell than in the precise waveforms.

To study the centring dynamics we focus on Z_s, the position of the geometrical

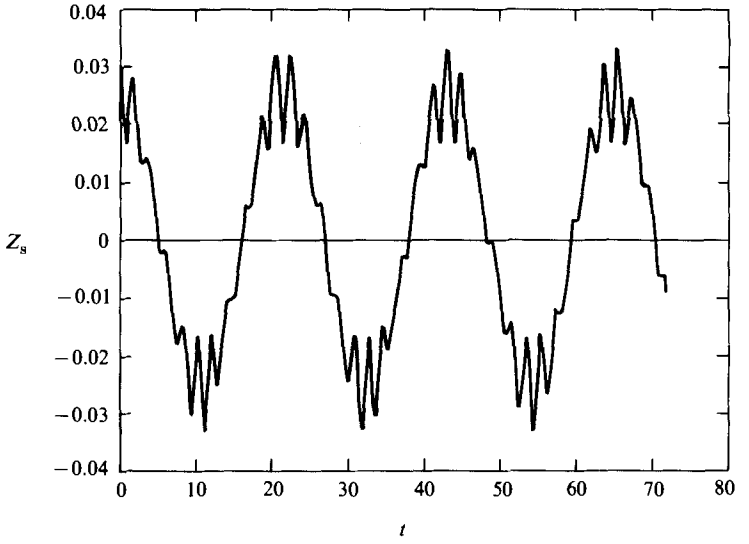

FIGURE 3. Centring for the $n = 2$ sloshing mode, $\epsilon = 0.5$, $\delta = 0.1$, $\Delta = 0.1$. Plot of Z_s versus t.

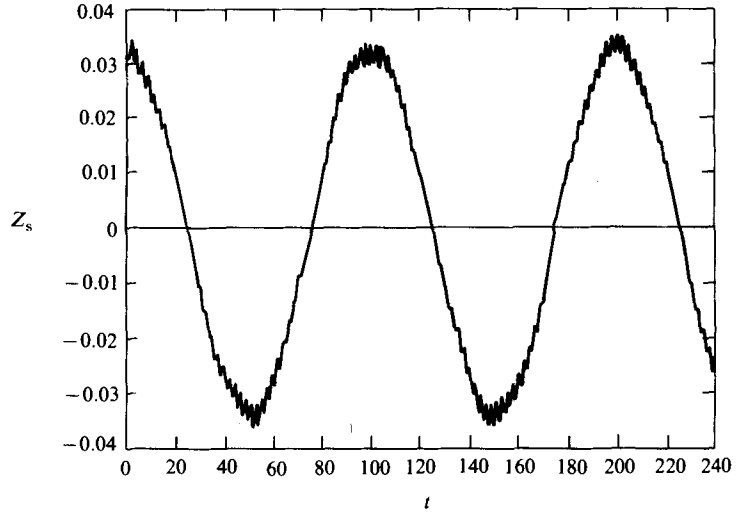

FIGURE 4. Centring for the $n = 2$ bubble mode, $\epsilon = 0.05$, $\delta = 0.1$, $\Delta = 0.1$. Plot of Z_s versus t.

centre relative to the centre of mass. Only the lowest ($n = 2$) modes will be considered.

For the sloshing mode we find that Z_s undergones a fast oscillation in time about some mean position as a linear consequence of the wave, and that this mean position in turn undergoes a slow oscillation in time about zero (which means the centre of mass) as a nonlinear consequence. Obviously the slow oscillation should be interpreted a a centring effect. In figure 3 we plot Z_s versus t for $\epsilon = 0.5$, $\delta = 0.1$, and $\Delta = 0.1$, and see that it behaves like a simple harmonic oscillator on the slow timescale.

For the bubble mode Z_s behaves similarly. In figure 4 we show Z_s versus t for

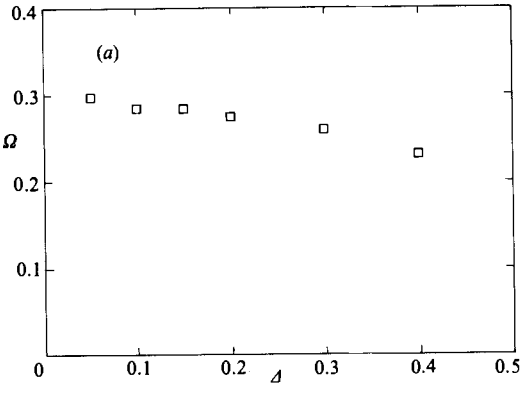

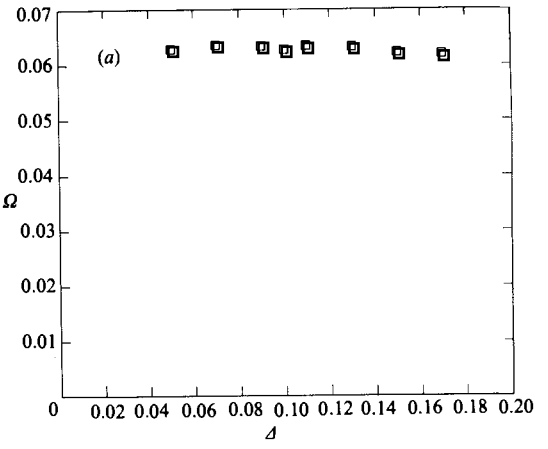

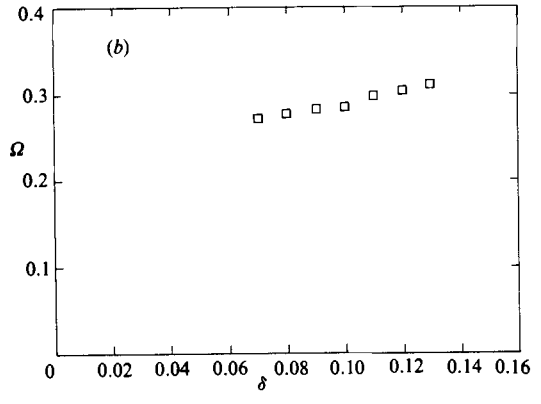

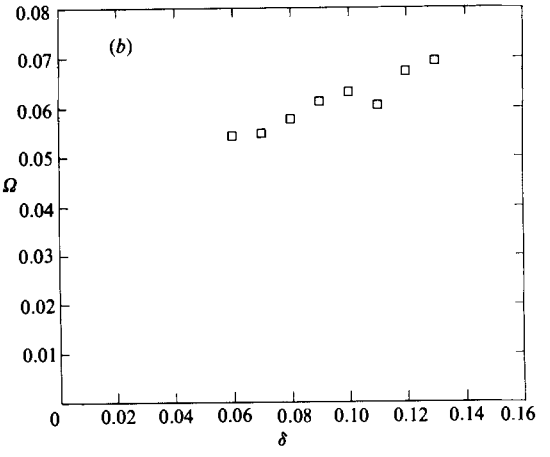

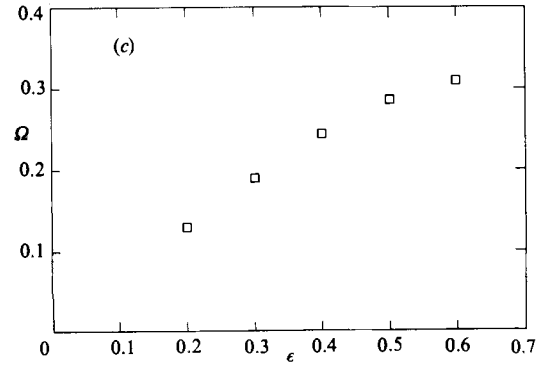

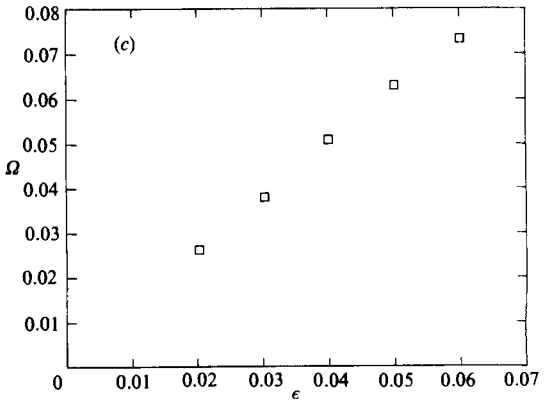

FIGURE 5.

FIGURE 6.

FIGURE 5. $n = 2$ sloshing mode: (*a*) Ω versus Δ, $\epsilon = 0.5$, $\delta = 0.1$; (*b*) Ω versus δ, $\epsilon = 0.5$, $\Delta = 0.1$; (*c*) Ω versus ϵ, $\delta = 0.1$, $\Delta = 0.1$.

FIGURE 6. $n = 2$ bubbles mode: (*a*) Ω versus Δ, $\epsilon = 0.05$, $\delta = 0.1$; (*b*) Ω versus δ, $\epsilon = 0.05$, $\Delta = 0.1$; (*c*) Ω versus ϵ, $\delta = 0.1$, $\Delta = 0.1$.

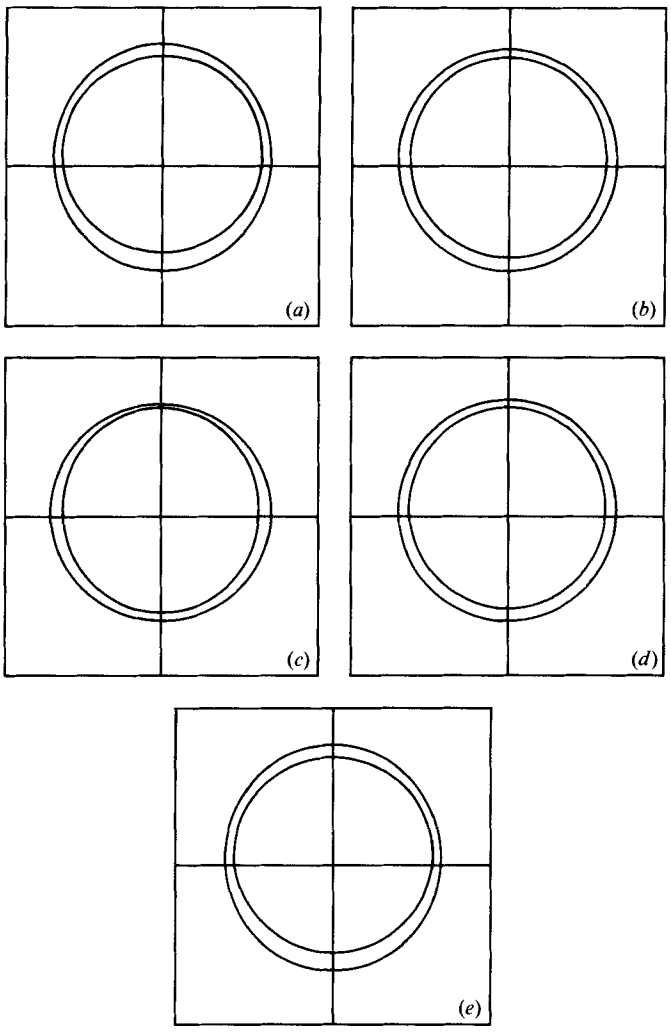

FIGURE 7. Typical wave profiles for the $n = 2$ sloshing mode of a non-concentric shell with origin at the centre of mass: $\epsilon = 0.5$, $\delta = 0.1$, $\Delta = 0.3$, dimensionless wave period $T = 1.8$. (*a*) $t = 0$, (*b*) $\frac{1}{4}T$, (*c*) $\frac{1}{2}T$, (*d*) $\frac{3}{4}T$, (*e*) T.

$\epsilon = 0.05$, $\delta = 0.1$, and $\Delta = 0.1$. It resembles figure 3 except that the ratio of the fast frequency to the slow one seems to be larger. For higher values of ϵ the program runs smoothly until at some point errors rapidly grow. The difficulty is numerical and occurs when the nonlinearity is too high, because then the spatial profile of the wave carries higher Legendre components, requiring more spatial grid points and a smaller time step.

The difficulty occurs for the bubble mode but not for the sloshing mode for the following reason. To compare the nonlinearity of the two modes we need to compare their wave amplitudes on the same basis. If we use ϵ to represent the amplitude of the sloshing mode, we have to use ϵ/δ for the bubble mode. Thus the waves described by figure 3 and figure 4 have comparable nonlinearity and energy. We cannot make the amplitude for the sloshing mode much higher because it is limited by the shell

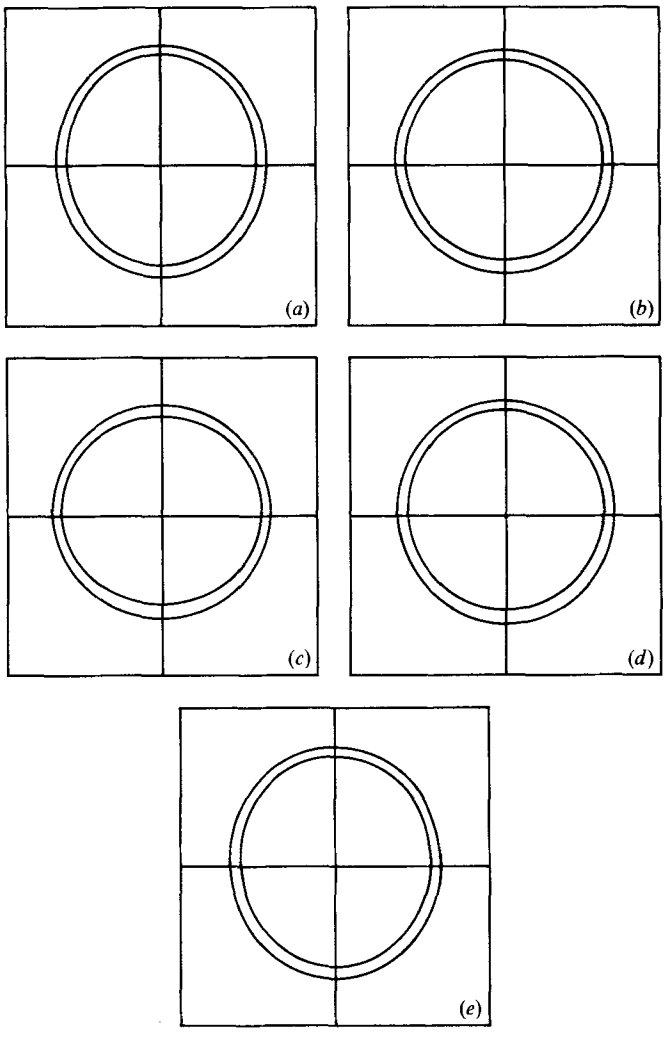

FIGURE 8. Typical wave profiles for the $n = 2$ bubble mode of a non-concentric shell with origin at the centre of mass: $\epsilon = 0.05$, $\delta = 0.1$, $\Delta = 0.15$, dimensionless wave period $T = 2.2$. (*a*) $t = 0$, (*b*) $\frac{1}{4}T$, (*c*) $\frac{1}{2}T$, (*d*) $\frac{3}{4}T$, (*e*) T.

thickness, but we can do so for the bubble mode, which leads to the numerical difficulty. In our earlier work (Lee & Wang 1986) the jet collapses fast enough, long before a numerical instability of this type can develop into a problem.

We seek to find the slow frequency Ω as a function of ϵ, δ, and Δ in a parameter study, by running the program repeatedly. Typically, for a given combination the run time for determining the slow oscillation pattern is about one day for the sloshing mode and a few hours for the bubble mode.

For the sloshing mode we first let $\epsilon = 0.5$ and $\delta = 0.1$, and run the program trying several values of Δ to look for the corresponding values of Ω. The results in figure 5 (*a*) show that when Δ is small Ω is independent of Δ. We conclude here that the slow oscillation obeys the linear Hooke's law, with deviation only when the core displacement is too large. We next let $\epsilon = 0.5$ and $\Delta = 0.1$, and run the program with

various values of δ to find the corresponding values of Ω. The results shown in figure 5(*b*) suggests that Ω is insensitive to δ as well. Finally we let $\delta = 0.1$ and $\Delta = 0.1$, and vary ϵ. The results in figure 5(*c*) indicate that Ω is proportional to ϵ:

$$\Omega = 0.6\epsilon, \tag{5.1}$$

where the constant can be obtained from the plot.

We show a similar sequence for the bubble mode in figure 6. In figure 6(*c*) the linear relation between Ω and ϵ is clear:

$$\Omega = 1.3\epsilon. \tag{5.2}$$

Higher modes require a finer spatial grid in the program and a longer run time. However, the main purpose of this investigation is to understand the physics of the system. As we shall see, this purpose can be served sufficiently by studying the lowest modes.

Finally, in figure 7(*a–e*) we show the profiles of a non-concentric shell in the $n = 2$ sloshing-mode oscillation in the first wave cycle. Similarly, in figure 8(*a–e*) we show those for the $n = 2$ bubble mode.

6. Viscous effects

In order to consider the effects of small viscosity we need the mathematical approach usually used in fluid mechanics. Our results in dimensional forms from the thin-sheet model will be adapted for this purpose.

For a free mass of liquid in air or a vacuum in the absence of gravity, using the Navier–Stokes equation and the continuity equation we can derive the energy principle

$$\frac{\mathrm{d}}{\mathrm{d}t}\left\{\int_V \mathrm{d}\boldsymbol{x}\,\tfrac{1}{2}\rho\boldsymbol{u}\cdot\boldsymbol{u} + \sigma\int_S \mathrm{d}a\right\} = -\tfrac{1}{2}\mu\int_V \mathrm{d}\boldsymbol{x}\left(\frac{\partial u_i}{\partial x_j}+\frac{\partial u_j}{\partial x_i}\right)\left(\frac{\partial u_i}{\partial x_j}+\frac{\partial u_j}{\partial x_i}\right), \tag{6.1}$$

where $\boldsymbol{u}$ and μ are the velocity field and the viscosity of the liquid, respectively, V is the volume of the liquid bounded by the surface S, $\mathrm{d}/\mathrm{d}t$ is the total time derivative, and summation convention is used in the tensor form on the right-hand side. In the bracket on the left-hand side the volume integral is the kinematic energy T of the liquid, and the surface integral is the potential energy U due to the presence of surface tension, such that the left-hand side represents the rate of change of the total energy of the liquid in time. The change is brought about by the viscous damping represented by the right-hand side, which is the negative of the dissipation function D. In the case of an oscillatory motion of the liquid we can evaluate the damping rate λ if the rate is much less than the oscillatory frequency. Following a method of Lamb (1945) we find the linear inviscid solution of the system, let it decay like $\exp(-\lambda t)$, substitute it into (6.1), average the equation over an oscillatory cycle and use the smallness of λ to obtain

$$\lambda = \langle D\rangle/4\langle T\rangle, \tag{6.2}$$

where $\langle\ \rangle$ means the average. In the following we study the damping of the wave and that of the core oscillation separately owing to their disparity in timescales.

First we note that the frequency of the wave is not sensitive to the position of the core, according to our numerical results here and our earlier analytical results using potential theory (unpublished). For damping, if the dissipation is increased by $O(\Delta)$ on one side of a non-concentric shell it must be decreased by the same on the other, such that the net correction to λ is at most of $O(\Delta^2)$. So if $\Delta \ll 1$, to study the damping

of the wave we can consider the shell as concentric. Similarly, we can argue that the errors in the frequency and damping rate of the wave due to neglecting nonlinearity are of $O(\epsilon^2)$.

For the wave the trial solution required to substitute into (6.2) can be found from potential theory. But we can obtain an approximate solution in the thin-shell limit from the available result of the thin-sheet model. For the sloshing mode v_s' is given by (4.6) and v_n' is zero in the model. To restore the potential flow we (*a*) let $u = 0$ and $v = v_s'$, both being considered as functions of r and θ; (*b*) require that $\nabla \cdot \boldsymbol{u} = 0$ to find u to $O(\xi)$ where we have defined $r = R_s + \xi$; (*c*) require that, $\nabla \times \boldsymbol{u} = 0$ to find the correction of v to $O(\xi)$; and finally (*d*) substitute u and v into (6.2) to find λ. The flow field is thus given to $O(\xi)$ by

$$u = -\epsilon\omega R_s \sin\omega t \frac{\xi}{R_s} P_n, \tag{6.3}$$

and

$$v = -\frac{\epsilon\omega R_s}{n(n+1)} \sin\omega t \frac{\partial P_n}{\partial\theta}\left(1 - \frac{\xi}{R_s}\right), \tag{6.4}$$

with the accuracies being sufficient for the evaluation of D, which involves only first derivatives of u and v with respect to ξ. They agree with the results of the potential theory (Saffren *et al.* 1982) in the thin-shell limit to $O(\xi)$. Putting (6.3) and (6.4) into (6.2) we find that

$$\lambda = \frac{\nu(2n^2+2n+1)}{R_s^2}, \tag{6.5}$$

where $\nu = \mu/\rho$ is the kinematic viscosity of the liquid.

In a similar manner for the bubble mode, starting with v_n' from (4.13) and neglecting v_s' of $O(\delta^2)$ from (4.14*b*) we find that

$$\lambda = \frac{2\nu(n^2+n+3)}{R_s^2}. \tag{6.6}$$

Thus, when viscosity is small but finite, the damping rate for either type of wave is proportional to ν/R_s^2, which is similar to that of a liquid drop in air (Lamb 1945).

Next we try to find the damping rate Λ of the core oscillation using an equivalent of (6.1). This effort is complicated by the fact that the slow frequency is proportional to the wave amplitude and therefore decays naturally. In this study we shall only consider the situation in which Ω is kept constant by maintaining a steady wave using an external excitation, e.g. a modulated sound field in acoustic levitation (Marsten & Apfel 1980). In the first trial assume as usual that Λ is much less than the core oscillation frequency Ω, so that we can use (6.2). As we have neither an explicit expression for the potential energy nor a 'linear inviscid' solution for the core motion we need to do some modelling. Let us imagine that the system is averaged over a wave cycle, so that the fast-changing part of the wave is filtered out but the average of its nonlinear effect remains in the form of a potential well to drive the core motion. The two interfaces can be considered as essentially spherical.

The linear slow-changing inviscid flow associated with the core motion is reconstructed as follows. Consider that $\mu = \mu_s(1 - \Delta\cos\theta)$ relative to the geometrical centre. If the origin is chosen to be at the stationary centre of mass, then μ relative to the origin is given approximately by the same expression and the geometrical centre is located at $Z_s = \frac{1}{3}\Delta R_s$, neglecting $O(\Delta^2)$. This relation between Δ and Z_s guarantees that the centre of mass remains stationary when Δ changes in time. The translational velocity of the geometrical centre along the z-axis is given by

$v_T = \frac{1}{3}R_s d\Delta/dt$. In the thin-sheet model the tangential and normal velocities are then $v_s = v_s' - v_T \sin\theta$ and $v_n = v_T \cos\theta$, respectively, neglecting $O(\Delta^2)$, where the presence of a correction v_s' in v_s is necessary so that μ, v_s and v_n may be consistent with the continuity equation (3.11). Since we expect the liquid to translate along the shell as the latter translates in order to maintain the centre of mass fixed, we correct v_s but not v_n. Using (3.11) and neglecting $O(\Delta^2)$, we find v_s' and obtain

$$v_s = \frac{1}{6}\frac{d\Delta}{dt} R_s \sin\theta, \tag{6.7}$$

and

$$v_n = \frac{1}{3}\frac{d\Delta}{dt} R_s \cos\theta. \tag{6.8}$$

To restore the potential flow we let $u = v_n$ and $v = v_s$. Applying $\nabla \cdot \boldsymbol{u} = 0$ and $\nabla \times \boldsymbol{u} = 0$ as before we find $\boldsymbol{u}$ to $O(\xi)$. As our numerical calculation has established that Δ is oscillatory we let $\Delta = \Delta_0 \cos\Omega t$.

The evaluation of the kinetic energy of the slow oscillation is easy; but that of the potential energy is non-trivial. However the latter is not necessary because for an oscillatory system $\langle T \rangle$ and $\langle U \rangle$ are equal except for a constant which comes from the equilibrium state and which can be set to zero, where now $\langle\ \rangle$ means averaging over a slow cycle. Thus for the core oscillation we find

$$\langle T \rangle = \langle U \rangle = \tfrac{1}{18}\pi\rho\Omega^2\Delta_0^2 R_s^4 D_s, \tag{6.9}$$

and

$$\langle D \rangle = \tfrac{10}{3}\mu\Omega^2\Delta_0^2 \pi R_s^2 D_s. \tag{6.10}$$

According to (6.2) the damping rate is thus

$$\Lambda = \frac{15\nu}{R_s^2}. \tag{6.11}$$

if the condition that Λ is much less than Ω is satisfied. Note that Λ is proportional to ν/R_s^2 too, but is independent of the mode type of the wave.

To check whether Lamb's method for the damping rate is indeed applicable we look at the numbers for a typical case. Let us consider a water shell with $\rho = 1$ gm cm^{-3}, $\sigma = 72$ dynes cm^{-1}, $\mu = 0.01$ gm cm^{-1} s^{-1}, $R_s = 0.1$ cm, and $D_s = 0.01$ cm. If the shell is in the $n = 2$ sloshing mode with a wave amplitude $\epsilon = 0.5$ we have $\omega = 294$ s^{-1} from (4.5), $f = \omega/2\pi = 47$ s^{-1}, $\lambda = 13$ s^{-1} from (6.5), $\Omega = 25$ s^{-1} from (5.1) (after multiplying its right-hand side by $\omega_0/\delta^{\frac{1}{2}}$ to obtain the dimensional form), $F = \Omega/2\pi = 4$ s^{-1}, and $\Lambda = 15$ s^{-1} from (6.11). If the shell is in the $n = 2$ bubble mode with $\epsilon = 0.05$ we have $\omega = 2400$ s^{-1} from (4.12), $f = \omega/2\pi = 382$ s^{-1}, $\lambda = 18$ s^{-1} from (6.6), $\Omega = 55$ s^{-1} from (5.2) (after multiplying its right-hand side by $\omega_0/\delta^{\frac{1}{2}}$ to obtain the dimensional form), $F = \Omega/2\pi = 9$ s^{-1}, and $\Lambda = 15$ s^{-1} as before. We observe that for the core oscillation the damping rate is only marginally smaller than the frequency, comparing Λ with Ω, implying that the use of Lamb's method is questionable.

However, we can remedy the shortcoming of our result by introducing a simple model. Let us consider T, U and D in (6.9) and (6.10) without averaging over a slow cycle $\langle\ \rangle$. Δ is then a function of t but no longer given by $\Delta_0 \cos\Omega t$. U is given by the right-hand side of (6.9) after replacing Δ_0^2 with $2\Delta^2$, assuming that it behaves like the potential well of a simple harmonic oscillator. T and D are given by the right-hand sides of (6.9) and (6.10) respectively after replacing $\Omega^2\Delta_0^2$ with $2(d\Delta/dt)^2$, since both depend on the square of the velocity field. Assuming that for the slow oscillation the

rate of change of the total energy $T+U$ is equal to $-D$, we find the equation for a damped harmonic oscillator. It has a solution for Λ of the form $\exp(-\alpha t)$ where

$$\alpha = \Lambda \pm (\Lambda^2 - \Omega^2)^{\frac{1}{2}}, \tag{6.12}$$

in which Λ is given by (6.11). When Λ is small enough such that the second term on the right-hand side of this formula is approximately equal to $i\Omega$, we recover our earlier result (6.11). For the typical case that we have considered we find that $\Lambda = \Lambda_0 \exp(-15t)\cos(21t)$ for the sloshing mode and $\Lambda = \Lambda_0 \exp(-15t)\cos(53t)$ for the bubble mode. These are not very different from those that we have obtained using Lamb's method. The frequency is not drastically changed by the viscosity in either case, and the core goes to the centre rapidly because the damping is indeed heavy, with the oscillations barely visible after a slow cycle or so. The objection may be raised that Ω and Λ are still too close for the viscous result to be valid. But it may also be argued, as we tend to believe, that since the improved model cannot produce much difference in this particular case, Lamb's method is a good approximation in spite of the shortcoming. However, this is only a reasonable conclusion without a rigorous basis.

More generally, (6.12) can be real or complex, depending on Ω, which is proportional to ϵ. If ϵ is small enough α becomes real and the core motion towards the centre of mass is purely exponential. The smaller ϵ is, the more slowly the centring occurs. If ϵ goes to zero one of the roots of α becomes zero and the core stays where it is. This simply means that without a wave there is no centring.

In the context of the present study, inviscid approximation is justified in the nonlinear regime if the Reynolds number, defined as $\omega\eta R_s/\nu$, is much greater than 1, where we have compared the inertial term with the viscous term in the momentum equation, and where η is the particle displacement amplitude of the wave of $O(\epsilon R_s)$ (see (4.6) or (4.13)). This criterion is the same as the damping rate for the slow oscillation in (6.11) being much smaller than the slow frequency in (5.1) or (5.2) in dimensional forms.

In experiments in which shell centring is observed, no one has ever systematically looked for and noticed any core oscillation. According to our model, core oscillation is a highly transient phenomenon because of viscosity. However, the inviscid result can be tested by first levitating the shell acoustically and maintaining a constant wave amplitude on it by modulating the sound to keep it from breaking. The core will be somewhat displaced upward by gravity. If we further impose a sinusoidal acceleration on the shell, e.g. by placing the whole apparatus on an oscillating platform, the core will oscillate up and down relative to the shell. The core oscillation should reach a resonance when the frequency of the platform is near those predicted by our theory.

7. Concluding discussion

According to our inviscid study the frequency ratio of the core and wave oscillations is proportional to the wave amplitude, and the ratio of their velocities is proportional to the core displacement amplitude. Thus to attack the problem using a perturbation analysis requires a lengthy multiparameter expansion in ϵ and Λ. On the other hand the thin-sheet model is conceptually simple and can be handled with a fairly simple program.

The algorithm that we have used is mostly *ad hoc*, but there are reasons to believe that the results are valid. First, we have been very careful to test whether the system

behaves correctly in predictable situations. Secondly, the results for the unknown situations of interest, i.e. those involving a non-concentric shell, are supported by the following physical picture.

For the $n = 2$ sloshing or bubble mode, if the core is displaced, the lighter side of the shell must oscillate harder to keep the centre of mass of the whole shell stationary in the absence of an external force. Therefore, on the average over a wave cycle the lighter side is a region of lower pressure according to the Bernoulli effect, causing the liquid to drift from the heavy side to the light side. As the force that causes the drift is opposite and arguably also proportional to the displacement, Hooke's law is the logical consequence. Therefore the drift is sinusoidal in time about the centre of mass rather than, say, exponential. Exponential behaviour can only come from viscosity. The same principle holds for higher modes.

Quantitatively, when the shell in oscillation is non-concentric, with the core displaced upward by Δ, the difference in Bernoulli pressure between the lower and the upper halves of the shell is of the order of $\frac{1}{2}\rho \boldsymbol{u} \cdot \boldsymbol{u}$ multiplied by Δ. Since $\boldsymbol{u}$ in both mode types is of $O(\omega\epsilon R_s)$ (see (4.6) and (4.13)), and the shell has a cross-sectional area of $O(R_s D_s)$, an internal force of $O(\rho\omega^2\epsilon^2 R_s^3 \Delta D_s)$ pushes the liquid upward. The corresponding acceleration of the liquid, which has a mass of $O(\rho D_s R_s^2)$, is of $O(-R_s \mathrm{d}^2\Delta/\mathrm{d}t^2)$, which is opposite in sign to the displacement as explained earlier. Using Newton's law and assuming that Δ is proportional to $\exp(-\mathrm{i}\Omega t)$ we find that Ω is of $O(\omega\epsilon)$. This result, if cast into dimensionless form, is consistent with (5.1) for the sloshing mode and (5.2) for the bubble mode.

In one of the experiments (Trinh 1983) the liquid shell is leviated acoustically against gravity without breaking. (Note that without support the shell undergoes a free fall and experiences a zero-gravity condition.) It is interesting to examine the strength of the centring mechanism versus that of gravity. With the shell prevented from falling, the buoyancy effect due to gravity tends to force the core to the top, leading to rupture of the shell. If the shell is in capillary oscillation, the light side at the top must oscillate harder than the heavy side even though there are external forces, otherwise the shell will exert an additional force on itself. Then, on the average over a wave cycle, the lower side has a Bernoulli pressure exceeding that of the upper side of the order of $\frac{1}{2}\rho \boldsymbol{u} \cdot \boldsymbol{u}$ times Δ, according to our earlier argument. In a dynamic equilibrium after the slow oscillation subsides, this difference must support the hydrostatic pressure due to gravity between the top and the bottom of the shell of the order of $\rho g R_s$. Since $\boldsymbol{u}$ is of the order of $\epsilon\omega R_s$, the equilibrium condition becomes

$$\Delta\epsilon^2 \sim \frac{g}{\omega^2 R_s}, \tag{7.1}$$

where g is taken as 980 cm s^{-2}. For the typical case we have mentioned $R_s = 0.1$ cm. In order that the shell does not break, Δ should be less than, or at most of the order of, one when a reasonable value of ϵ is used. For the $n = 2$ sloshing mode $\omega = 295$ s^{-1} and $\epsilon = 0.5$ such that $\Delta \sim 0.5$, which is less than one. For the $n = 2$ bubble mode $\omega = 2400$ s^{-1} and $\epsilon = 0.05$ such that $\Delta \sim 0.7$, which is still within the safety margin. Therefore the centring mechanism is strong enough to support the liquid shell against the action of gravity.

Finally in figures 5(*b*) and 6(*b*) the slow frequency seems to increase slightly with δ. But the model cannot take into account the fact that the flow also becomes less uniform across the thickness. Higher-order corrections in δ are then required. In the extreme case in which the shell is so thick that the core is like a bubble in an infinite medium one can easily imagine that the centring force is non-existent. But it has

been demonstrated that in a thick shell levitated acoustically against gravity, the core floating to the top can remain submerged below a thin layer of liquid if the shell is excited into a strong resonant oscillation (E. Trinh 1984, private communication). Vigorous capillary wave motion is visible on the layer, while the rest of the shell is relatively quiescent. The distribution of wave activity in the shell is consistent with our notion that the lighter side oscillates harder. Although the thin-shell model is no longer valid here, our physical picture is still applicable. However, in this case the effect is strong only when the bubble is close to the surface. It prevents the bubble from escaping the drop, but lacks the strength to really push the bubble towards the centre. If one agrees that 'centring' means the tendency for the core to go to the centre, then it is more appropriate to call this situation 'trapping' rather than 'centring' of the bubble. It is therefore reasonable to say that centring is less effective when the shell is thick.

This work represents one phase of research carried out at the Jet Propulsion Laboratory, California Institute of Technology, Pasadena, under contract with the National Aeronautics and Space Administration. We are grateful to Dr E. Trinh for showing us the video tapes of his experiment, some of which have not been published. We also wish to thank Dr J. Kendall for his comments, and Mr J. Wilson for editing the manuscript.

REFERENCES

JOHNSON, R. E. & SADHAL, S. S. 1985 Fluid mechanics of compound multiphase drops and bubbles. *Ann. Rev. Fluid Mech.* **17**, 289–320.

KENDALL, J. M. 1986 Experiments on annular liquid jet instability and on the formation of liquid shells. *Phys. Fluids* **29**, 2086–2094.

LAMB, H. 1945 *Hydrodynamics*, 6th edn. Dover.

LEE, C. P. & WANG, T. G. 1986 A theoretical model for the annular jet instability. *Phys. Fluids* **29**, 2076–2085.

LEE, H. C. 1974 Drop formation in a liquid jet. *IBM J. Res. Develop.* **18**, 364–369.

LEE, M. C., FENG, I. A., ELLEMAN, D. D., WANG, T. G. & YOUNG, A. T. 1982 Generation of a strong core centering force in a submillimeter compound droplet system. In *Proc. Second Intl Colloquium on Drops and Bubbles, Monterey, California, November 1981* (ed. D. H. Le Croissette) (*Jet Propulsion Laboratory Publication* 82–7), pp. 107–111.

LEE, M. C., KENDALL, J. M., BAHRAMI, P. A. & WANG, T. G. 1986 Sensational spherical shells. *Aerospace Am.* **24**, 72–76.

MARSTON, P. & APFEL, R. 1980 Quadrupole resonance of drops driven by modulated acoustic radiation pressure–experimental properties. *J. Acoust. Soc. Am.* **67**, 27–37.

SAFFREN, M., ELLEMAN, D. D. & RHIM, W. K. 1982 Normal modes of a compound drop. In *Proc. Second Intl Colloquium on Drops and Bubbles, Monterey, California, November 1981* (ed. D. H. Le Croissette) (*Jet Propulsion Laboratory Publication* 82–7), pp. 7–14.

TAYLOR, G. I. 1959 The dynamics of thin sheets of fluid: II. Waves on fluid sheets. *Proc. R. Soc. Lond.* A **253**, 296–312.

TRINH, E. 1983 Fluid dynamical studies of free liquids using acoustic levitation. *Ultrasonic Symp.* (ed. B. McAvoy), vol. 2, pp. 1143–1146. IEEE.

ZABUSKY, N. J. 1984 Computational synergetics. *Phys. Today* **37**, 36–45.